Effect of Detuning on the Development of Marginally Unstable Baroclinic Vortices

PIERRE GAUTHIER

Division de Recherche en Prévision Numérique, Atmospheric Environment Service, Dorval, P.Q., Canada

(Manuscript received 24 July 1989, in final form 22 November 1989)

ABSTRACT

This paper is concerned with the weakly nonlinear inviscid dynamics of a marginally unstable baroclinic wave near the point of minimum critical shear of a two-layer quasi-geostrophic model on the β-plane. In previous studies by Pedlosky and by Warn and Gauthier (WG), the parameters of the model were chosen in a specific way in order to be exactly at the minimum. They showed that at this particular point, a complete inviscid coarse-grain homogenization of the potential vorticity occurs in the bottom layer causing the amplitude of the unstable wave to equilibrate. It is the purpose of the present paper to investigate the behavior of the dynamics when the problem is not exactly at the minimum and more specifically, to establish how one goes from the analytical solution of WG to the single wave theory that one expects to be valid away from minimum critical shear. The nonlinear evolution equations of WG are extended in order to include a "detuning parameter" σ associated with a perturbation of the aspect ratio of the periodic channel. An analytical solution not being available when $\sigma \neq 0$, a spectral form of these equations similar to those found in Pedlosky is integrated numerically at high resolution. The results show that for a fixed supercritical shear and arbitrary but sufficiently small initial conditions, the size of the vortices is decreasing with σ causing the potential vorticity to mix only in part of the domain and the amplitude of the unstable wave to oscillate around a nonzero mean. When σ is sufficiently large, closed streamlines are no longer possible and no vortices are developing. At that point, the single wave theory is becoming a better approximation to the dynamics.

1. Introduction

One of the main characteristics of atmospheric motion at middle latitudes is the emergence of synoptic scale vortices in a flow that has initially a nearly zonal configuration. By considering quasi-geostrophic models, Charney (1947) and Eady (1949) concluded that the development of these systems could be explained by a hydrodynamic instability that is now called *baroclinic instability* in which the growth of the perturbation occurs through an energy transfer from the zonal part of the flow towards synoptic-scale perturbations.

By creating a transport of heat and angular momentum, these perturbations modify in turn the configuration of the large-scale circulation by decreasing the meridional temperature gradient. In general circulation models, there is a need for a good parameterization of these transports. One such parameterization has been proposed by Stone (1978) who formulated the idea of baroclinic adjustment by which these transports constantly bring back the mean zonal flow to a neutral configuration. However, as was pointed out by Vallis (1988), the nonlinearity of the problem can sometimes lead to an equilibrated state for which the mean zonal flow may be quite different from a neutral basic state. The dynamics underlying this kind of development and in particular the role of the nonlinearity is still not understood.

The simplest model that can be used to study baroclinic instability is the quasi-geostrophic two-layer model introduced by Phillips (1954). Linearizing the governing equations, the solutions can be formulated in terms of normal modes of the form $e^{-ikct}\phi(x, y)$ which are *unstable* when $\mathrm{Im}\{c\} > 0$. In order to be able to develop a weakly nonlinear theory, the parameters of the model must be chosen in such a way that the growth rate of the unstable wave is small. The weak instability then acts on a slow time scale. Eventually, the amplitude of the unstable wave approaches a small but finite value. In that case, the flow remains close to the basic state and the process of linearization is still meaningful. This has been studied first by Pedlosky (1970) and afterwards by many other authors who investigated this question in different contexts: the review paper by Hart (1979) gives an extensive bibliography.

When relatively strong dissipation is present, the dimension of the dynamical system can be reduced to one that retains only the neutral and unstable modes while the stable modes are entirely determined by those modes. This is justified in bifurcation theory by the *center manifold theorem* (Guckenheimer and Holmes 1983). The low-order models are correct in this context but difficulties arise when dissipation becomes weak. Moreover, the two-layer model is structurally unstable

Corresponding author address: Dr. Pierre Gauthier, Division de Recherche en Prévision Numérique (A.E.S.), 2121 Transcanadian Highway, Dorval, P.Q., Canada H9P 1J2.

to weak dissipation in the sense that its behavior is extremely dependent on the type of dissipation used. For instance, Holopainen (1961) and later Newell (1972) and Romea (1977) pointed out that when symmetric Ekman pumping is introduced in a β-plane model, the inviscid limit of the neutral curve differs from the inviscid neutral curve. But this behavior disappears when potential vorticity dissipation is used (Pedlosky 1982b).

To avoid the structural instability associated with weak dissipation, one has to turn to the inviscid model for which stable modes are in fact neutral. Consequently, when forced through nonlinear interactions, they do not disappear and are in a position to influence the dynamics of the problem. However, it is intuitively possible to consider only the neutral modes that interact resonantly with the weakly unstable wave. One can argue that the results obtained in this manner are an accurate description of the evolution for intermediate times although the long term behavior could only be determined by considering also the nonresonant interactions.

Being interested in midlatitude atmospheric motion, the inviscid model considered in the present paper is formulated on the β-plane and the flow is confined within a periodic channel (in x) bounded by rigid walls located at $y = 0, 1$. If the basic state is one of constant but different zonal winds in the two layers (referred to as Phillips' model in the literature), a linear stability analysis (see Pedlosky 1979) shows that a minimum vertical shear is required to trigger instability. As in Pedlosky (1982a,b) and Warn and Gauthier (1989, WG hereafter), the problem is set in the vicinity of the point of minimum critical shear, which is of particular interest when the wavenumber is continuously varying as in the wavepacket problem introduced by Pedlosky (1972), for instance.

As stated in Pedlosky (1982a), when the problem is set on the neutral curve but away from minimum critical shear, the single wave theory of Pedlosky (1970) should apply, the amplitude of the unstable wave $S(T)$ would be governed by

$$\frac{d^2S}{dT^2} = S(\delta - |S|^2)$$

and $S(T)$ would have an oscillatory behavior. On the other hand, when it is set exactly at minimum critical shear, Pedlosky (1982a,b) showed that the marginally unstable wave is interacting resonantly with an infinite number of nondispersive modes. Instead of solving numerically for a finite set of these as Pedlosky did, Warn and Gauthier reformulated the problem in such a way as to make it possible to solve it analytically. This solution enabled them to show that $S(T)$ equilibrates to a constant value due to the coarse-grain homogenization of the potential vorticity that occurs in the bottom layer. In this paper, the geometry of the channel is perturbed as to be slightly off the minimum. This allows us to move on the neutral curve to investigate how one goes from the solution of WG to the single wave theory. When the wavenumber is such that the problem is exactly set at the minimum of the neutral curve, the linear phase speed of the unstable wave is exactly tuned to the one of the non-dispersive modes. By moving away from this point, the phase speed of the unstable wave starts to differ slightly from the one of the nondispersive modes: we will refer to this effect as the "detuning effect" caused by the perturbation to the aspect ratio of the channel.

In the next section, the results of the linear stability analysis at the point of minimum critical shear are recalled. In section 3, the derivation of the nonlinear evolution equations presented in WG is generalized to add the detuning effect. In the present case, it will not be possible to solve analytically as in WG. In section 4, the spectral form of these evolution equations is given and it is also shown that energy and potential enstrophy are conserved for certain truncated sets of spectral modes. The results obtained from the numerical integrations at high resolution are presented in section 5. If σ is a measure of the detuning, the vortices which occupy the whole domain when $\sigma = 0$ gradually shrink as σ is increased and eventually disappear when σ is sufficiently large: in that case, the flow can be described relatively well by the single wave theory. In appendix A, the conservation of energy is expressed in terms of the spectral components while in appendix B, it is shown that potential enstrophy and energy are conserved when the "truncation order" is even (see section 5).

2. Description of the model

As in WG, we consider the inviscid quasi-geostrophic motion of two layers of homogeneous stably stratified immiscible fluids rotating with angular velocity 2Ω. The variation of the Coriolis parameter is taken into account by making the β-plane approximation i.e. $2\Omega = f_0 + \beta' y'$. The flow is confined within a periodic channel of width L_y and length L_x and is bounded above and below by horizontal planes a distance D apart. When at rest, the two layers have equal depths (see Pedlosky 1970, 1979 for a complete description of the two-layer model).

The subscripts $n = 1, 2$ referring to the upper and bottom layer respectively, the governing nondimensional equations are the potential vorticity equations

$$\frac{\partial Q_n}{\partial t} + J(\psi_n, Q_n) = 0, \tag{1}$$

where ψ_n is the streamfunction, $J(f, g) = f_x g_y - f_y g_x$ the Jacobian while

$$Q_n = \nabla^2\psi_n + (-1)^n F(\psi_1 - \psi_2) + \beta y$$

is the absolute potential vorticity of the corresponding

layer. The rotational Froude number F and the parameter β are defined as

$$F = \frac{f_0^2 L_y^2}{(\Delta\rho/\rho_2)gD/2}, \quad \beta = \beta' L_y^2/U^*,$$

U^* being a typical velocity scale, g the gravitational acceleration and $\Delta\rho = (\rho_2 - \rho_1) > 0$, the density difference between the two layers. On the side walls located at $y = 0, 1$, the boundary conditions are

$$\frac{\partial\psi_n}{\partial x} = 0, \quad \int_0^L \frac{\partial^2\psi_n}{\partial t\partial y}\, dx = 0,$$

where $L = L_x/L_y$ is the aspect ratio of the channel (Phillips 1954).

Considering a purely baroclinic basic state, the streamfunction is rewritten as

$$\psi_n = -U_n y + \mu\phi_n,$$

with $\phi_n \sim O(1)$, the parameter $\mu \ll 1$ characterizing the initial amplitude of the disturbance. The linearized form of (1) is then

$$\left(\frac{\partial}{\partial t} + U_T\frac{\partial}{\partial x}\right)\zeta_1 + (\beta + FU_T)\frac{\partial}{\partial x}\phi_1 = 0$$

$$\frac{\partial}{\partial t}\zeta_2 + (\beta - FU_T)\frac{\partial}{\partial x}\phi_2 = 0, \qquad (2)$$

where

$$\zeta_n = \nabla^2\phi_n + (-1)^n F(\phi_1 - \phi_2)$$

is the perturbation potential vorticity. Without loss of generality, U_2 has been set to zero and $U_1 \equiv U_T$ is the vertical shear of the basic state. Solutions of the form

$$\phi = \begin{bmatrix}\phi_1\\ \phi_2\end{bmatrix} = \alpha\begin{bmatrix}1\\ \gamma\end{bmatrix}\frac{e^{ik(x-ct)}}{2}\sin N\pi y + \text{C.C.}$$

to (2) are possible if the dispersion relation

$$c_\pm = \frac{U_T}{2} - \frac{\beta(a^2+F)}{a^2(a^2+2F)} \pm \frac{1}{2a^2(a^2+2F)} \times [4\beta^2F^2 - U_T^2a^4(4F^2 - a^4)]^{1/2} \qquad (3)$$

is satisfied and

$$\gamma(c_\pm) \equiv \gamma_\pm = \frac{(a^2+F)}{F} - \frac{\beta + FU_T}{F(U_1 - c_\pm)}.$$

Here, C.C. stands for complex conjugate, $a^2 = k^2 + N^2\pi^2$ is the square of the total wavenumber while $k = 2\pi/L$.

As in Pedlosky (1982a,b) and WG, the problem is set in the vicinity of the point of minimum critical shear by letting

$$U_T = \frac{\beta}{F} + \Delta, \qquad (4)$$

with $\Delta \ll 1$.

The linear properties of this model when $U_T = \beta/F$ are very particular. For instance, the dispersion relation shows that the two vertical modes are such that

$$c_- = 0, \quad \gamma_- = \frac{(a^2 - F)}{F},$$

$$c_+ = \frac{\beta(a^4 - 2F^2)}{a^2F(a^2+2F)}, \quad \gamma_+ = \frac{F}{(a^2+F)},$$

the first one (c_-) being nondispersive. The potential vorticity associated with these two modes is

$$\zeta_{1-} = -2F\phi_{1-}, \quad \zeta_{2-} = -\frac{(a^4 - 2F^2)}{F}\phi_{1-},$$

$$\zeta_{1+} = -\frac{a^2(a^2+2F)}{(a^2+F)}\phi_{1+}, \quad \zeta_{2+} = 0, \qquad (5)$$

implying that only the nondispersive modes possess potential vorticity in the bottom layer.

If $(\pi^2\sqrt{2})/2 < F < 2\sqrt{2}\pi^2$, only the gravest meridional mode ($N = 1$) can be unstable at minimum critical shear and a particular aspect ratio $L = L_m$ is required since

$$a_m^2 = k_m^2 + \pi^2 = \sqrt{2}F$$

where $k_m = 2\pi/L_m$. The mode for which $a^2 = \sqrt{2}F$ is marginally stable is of the form

$$\phi = \left\{\alpha_1\begin{bmatrix}1\\ \gamma_m\end{bmatrix} + \alpha_2\begin{bmatrix}t\\ \Gamma + \gamma_m t\end{bmatrix}\right\}\frac{e^{ikx}}{2}\sin\pi y + \text{C.C.},$$

where $\gamma_m = \sqrt{2} - 1$ and $\Gamma = 2F/i\beta k_m$. Because of the linear growth in time, this behavior has been called "direct resonance" by Akylas and Benney (1980, 1982) who pointed out that it can act as a selection mechanism which results in the dominance of a single mode in the leading order solution (see the discussion in WG). As t becomes large,

$$\phi \to \alpha_2 t\begin{bmatrix}1\\ \gamma_m\end{bmatrix}\frac{e^{ik_m x}}{2}\sin\pi y + \text{C.C.} \qquad (6)$$

Even though the primary wave eventually dominates the flow configuration, linear theory indicates that the order of magnitude of the potential vorticity in the bottom layer associated with this wave is determined by the initial conditions and a detailed description of it requires the non-dispersive modes to be retained. This may also be seen by noting that these modes interact resonantly with the primary wave.

In the present study, the problem will be set "off resonance" by letting $L = L_m + \lambda$ with $\lambda \ll 1$. The zonal wavenumber is then $k \approx k_m + K$ while

$$a^2 = \sqrt{2}F + 2k_mK + O(K^2), \qquad (7)$$

where $K = -(2\pi/L_m^2)\lambda \ll 1$. From (4), (7) and the dispersion relation, the neutral curve is characterized by the relation

$$\Delta \sim 4\frac{\beta k_m^2}{F^3}K^2, \tag{8}$$

to leading order in K and Δ. If both effects are to intervene at the same order, K must be of $O(\Delta^{1/2})$ in which case, the real part of the phase speed is

$$c_R \sim (2-\sqrt{2})\frac{\beta k_m}{F^2}K. \tag{9}$$

The presence of K both modifies the level of the critical shear as well as the phase speed of the unstable wave. Moreover, the dispersion relation and (4) indicate that the nondispersive modes have a phase speed of $O(\Delta)$ and are therefore slower. This implies that the resonant interaction between these modes and the primary wave is weakened and K will consequently be referred to as the "detuning parameter".

If ϵ is a measure of the amplitude of the unstable wave in its nonlinear stage, it will be seen in the next section that the appropriate slow time scale is $\tau = \epsilon t$. By choosing $\Delta \sim O(\epsilon^2)$ and $K \sim O(\epsilon)$, these effects will also be perceived on this time scale.

3. Derivation of the nonlinear evolution equations

The asymptotic development of WG is now generalized to include the detuning effect. If $\epsilon \ll 1$, the streamfunction is expanded as

$$\psi_n = -U_n y + \epsilon\phi_n;$$

U_2 having been set to zero, the solutions depend on the slow time scale $\tau = \epsilon t$ alone. To act on this time scale, the vertical shear is $U_T = \beta/F + \epsilon^2\delta'$ while the detuning parameter is chosen to be $K = \epsilon K'$. From now on, K will stand for K'.

The easiest way to introduce the detuning in the problem is to define the new variable $X = kx$ and to let $k = k_m + \epsilon K$. Derivatives with respect to x are then expanded as

$$\frac{\partial}{\partial x} = (k_m + \epsilon K)\frac{\partial}{\partial X},$$

$$\frac{\partial^2}{\partial x^2} = (k_m^2 + 2\epsilon k_m K + \epsilon^2 K^2)\frac{\partial^2}{\partial X^2}.$$

Expanding ϕ_n as

$$\phi_n \sim \psi_n^{(0)} + \epsilon\psi_n^{(1)} + \cdots,$$

the leading order problem is

$$\frac{\beta k_m}{F}\frac{\partial}{\partial X}(\nabla_m^2\psi_1^{(0)} + F(\psi_1^{(0)} + \psi_2^{(0)})) = 0, \tag{10}$$

$$\frac{\partial}{\partial \tau}\zeta_2^{(0)} + J(\psi_2^{(0)}, \zeta_2^{(0)}) = 0, \tag{11}$$

with $\zeta_N = \nabla_m^2\psi_N + (-1)^N F(\psi_1 - \psi_2)$ and $\nabla_m^2 = k_m^2(\partial^2/\partial X^2) + (\partial^2/\partial y^2)$.

As discussed earlier, the leading order solution is taken to be the primary wave alone and consequently,

$$\psi^{(0)} = A(\tau)\begin{bmatrix}1\\ \gamma_m\end{bmatrix}\frac{e^{iX}}{2}\sin\pi y + \text{C.C.} \tag{12}$$

Even though it is a fully nonlinear equation, (11) is trivially satisfied at this order because $\zeta_2^{(0)} = 0$.

This solution has to be properly matched to the early time behavior, which is given by (6). For $\tau \ll 1$, (6) and (12) give

$$\alpha_2 t = \frac{\alpha_2\tau}{\epsilon} \approx \epsilon(A(0) + \tau A_\tau(0)).$$

This can be only if $A(0) = 0$ while $A_\tau(0)$ is arbitrarily defined by the initial conditions. This also shows that while the primary wave grows up to $O(\epsilon)$, all the other modes remain behind with an amplitude which is at most of $O(\epsilon^2)$. Consequently, they would have to be introduced at higher order. The reader is referred to WG and Akylas and Benney (1980, 1982) for a complete discussion of this point.

At the next order, the top-layer equation gives

$$\frac{\beta k_m}{F}\frac{\partial}{\partial X}(\nabla_m^2\psi_1^{(1)} + F(\psi_1^{(1)} + \psi_2^{(1)}))$$
$$= -\frac{\partial}{\partial\tau}\zeta_1^{(0)} - 2\frac{\beta k_m^2}{F}K\psi_{1XXX}^{(0)}$$
$$= 2F\left[\frac{dA}{d\tau} + iK\frac{\beta k_m^2}{F^2}A\right]\frac{e^{iX}}{2}\sin\pi y + \text{C.C.}, \tag{13}$$

while the bottom-layer one yields

$$\frac{\partial}{\partial\tau}(\zeta_2^{(1)} + 2k_m K\psi_{2XX}^{(0)}) + k_m J(\psi_2^{(0)}, \zeta_2^{(1)} + 2k_m K\psi_{2XX}^{(0)}) - \delta' F k_m\frac{\partial}{\partial X}\psi_2^{(0)} = 0. \tag{14}$$

The absolute potential vorticity of the bottom layer being $Q_2 = \epsilon^2 Q'(X, y, \tau)$ with

$$Q' = \zeta_2^{(1)} + 2k_m K\psi_{2XX}^{(0)} - \delta' F y,$$

(13) can be rewritten as

$$\frac{\partial Q'}{\partial\tau} + k_m J(\psi_2^{(0)}, Q') = 0. \tag{15}$$

The definition of $Q'(X, y, \tau)$ implies that

$$\nabla_m^2\psi_2^{(1)} + F(\psi_1^{(1)} - \psi_2^{(1)})$$
$$= Q' + 2Kk_m\gamma_m\left[A\frac{e^{iX}}{2} + \text{C.C.}\right]\sin\pi y + \delta' F y, \tag{16}$$

while integrating (13) with respect to X gives

$$\nabla_m^2\psi_1^{(1)} + F(\psi_1^{(1)} + \psi_2^{(1)}) = -i\frac{2F^2}{\beta k_m}\left[\frac{dA}{d\tau} + iK\frac{\beta k_m^2}{F^2}A\right]\frac{e^{iX}}{2}\sin\pi y + \text{C.C.} + g(y, \tau) \tag{17}$$

g being an arbitrary function of y and τ. Since $(1, \gamma_m)^T e^{iX} \sin\pi y$ is a solution to the homogeneous form of (16) and (17), these equations can only be solved if the following solvability condition is satisfied:

$$\frac{dA}{d\tau} + iK\frac{\beta k_m^2}{F^2}(1+\gamma_m^2)A = -4i\frac{\beta k_m}{F^2}\gamma_m\left\langle Q'\frac{e^{-iX}}{2}\sin\pi y\right\rangle \quad (18)$$

where $\langle \ldots \rangle$ denotes the average over the whole domain i.e.

$$\langle \cdots \rangle = \frac{1}{2\pi}\int_0^{2\pi} dX \int_0^1 (\cdots)\, dy.$$

The new variables

$$Q = \pi(Q' + \delta' F/2), \quad Y = \pi\left(y - \frac{1}{2}\right), \quad \delta = \delta' F,$$

$$T = \gamma_m k_m \left(\frac{2\beta}{F^2}\right)^{1/2}\tau, \quad S = \left(\frac{F^2}{2\beta}\right)^{1/2}\pi A,$$

bring (15) and (18) in the following final form:

$$\frac{\partial Q}{\partial T} + J(\Phi, Q) = 0, \quad (19)$$

$$\frac{dS}{dT} + i\sigma S = -2i\langle QW_0^*\rangle, \quad (20)$$

where

$$\Phi = SW_0 + \text{C.C.}, \quad W_0 = \frac{1}{2}e^{iX}\cos Y,$$

$$\sigma = 2Kk_m\left(\frac{\beta}{F^2}\right)^{1/2}.$$

When $\sigma = 0$, the unstable wave is located exactly at the minimum and our (19) and (20) then correspond to (19) and (20) of WG when the dissipation ν vanishes in their equations.

Expressing (8) in terms of these new variables, the neutral curve is locally defined by the relation $\delta_c = \sigma^2$ while from (9), the linear phase speed is $C_R = \sigma/2$. We will now prove that (19) and (20) imply that the unstable wave always travel at its linear phase speed. By differentiating (20) with respect to T and using (19), one obtains that

$$\frac{d^2S}{dT^2} + i\sigma\frac{dS}{dT} = -2S\langle |W_0|^2 Q_Y\rangle. \quad (21)$$

The effect of the linear phase speed can be removed by making the substitution

$$S(T) = R(T)e^{-i\sigma T/2}$$

in (21) which becomes

$$\frac{d^2R}{dT^2} + \frac{\sigma^2}{4}R = -\frac{R}{2}\langle Q_Y \cos^2 Y\rangle. \quad (22)$$

By translating the X coordinate, dR/dT can be chosen to be real and positive initially. Since $R(0) = 0$, the fact that (22) has real coefficients implies that $R(T)$ will remain real for all times. Consequently, the primary wave is moving at the linear phase speed.

It is then appropriate to use the new coordinate $\xi = X - \sigma T/2$, which bring (19) and (20) in the following form:

$$\frac{\partial Q}{\partial T} - \left(\frac{\sigma}{2} + R\Psi_Y\right)\frac{\partial Q}{\partial \xi} + R\Psi_\xi\frac{\partial Q}{\partial Y} = 0, \quad (23a)$$

$$\frac{dR}{dT} = +\langle Q\Psi_\xi\rangle, \quad (23b)$$

where $\Psi = \cos\xi\cos Y$. Equation (23a) indicates that the detuning adds a constant zonal component to the streamfunction. When $\sigma = 0$, the streamfunction has the configuration shown in Fig. 1a and variations in $R(T)$ result only in changes in the intensity and direction of the flow. Because of this, an exact solution can be found for this case (see WG). However, when $\sigma \neq 0$, the flow configuration varies with the ratio $\sigma/2R$. To show this effect, the streamfunction has been represented for particular values of this ratio on Fig. 1. The circulation has both open and closed streamlines and an analytical solution does not seem to be possible since variations of $R(T)$ will result in different flow configurations.

In the next section, a spectral form of (19) and (20) is presented. It will be integrated to investigate the behavior of the unstable wave and of the vorticity field when $\sigma \neq 0$. For the 'subliminal case' of WG, $Q(X, Y, 0) \approx -\delta Y$ and the development of strong gradients in the vorticity field implies that due to the finite spatial resolution, any numerical solution would be valid only for a finite period of time. An analytical solution being available, it will be useful to test the accuracy of the numerical ones.

4. The spectral equations

If Q is replaced by $\zeta - \delta Y$, (19) and (20) become

$$\frac{\partial \zeta}{\partial T} + J(\Phi, \zeta) - \delta\Phi_X = 0, \quad (24)$$

$$\frac{dS}{dT} + i\sigma S = -2i\langle \zeta W_0^*\rangle. \quad (25)$$

Next, the perturbation potential vorticity ζ is expanded as

$$\zeta = 4\sum_{m,n} B_{m,n}\frac{e^{imX}}{2}\sin n(Y + \pi/2), \quad (26)$$

where the notation

$$\sum_{m,n} \equiv \sum_{m=-\infty}^{+\infty}\sum_{n=1}^{\infty}$$

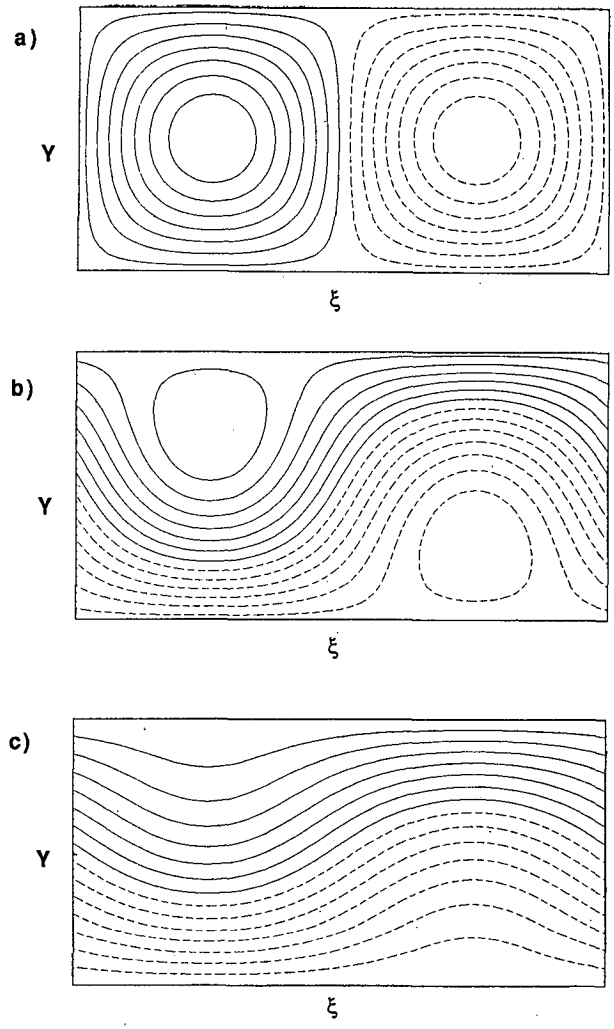

FIG. 1. Representation of the streamfunction

$$\psi = \frac{\sigma}{2} Y + R(T) \cos\xi \cos Y$$

when (a) $\sigma/2R = 0$, (b) $\sigma/2R = 0.6$, (c) $\sigma/2R = 1.5$. The domain is such that $-\pi/2 < \xi < 3\pi/2$ and $-\pi/2 < Y < \pi/2$. Dashed lines indicate negative values.

has been used. Using the fact that

$$J\left(\frac{e^{\pm iX}}{2}\sin(Y+\pi/2), \frac{e^{imX}}{2}\sin n(Y+\pi/2)\right)$$
$$= -\frac{i}{8} e^{i(m\pm1)X}[(m \pm n)\sin(n-1)(Y+\pi/2) + (m \mp n)\sin(n+1)(Y+\pi/2)],$$

the introduction of (26) in (24) yields the following result:

$$\frac{d}{dT}B_{m,n} = \frac{i}{4}[(m+n)(SB_{m-1,n+1} + S^*B_{m+1,n-1}) + (m-n)(SB_{m-1,n-1} + S^*B_{m+1,n+1})], \quad (27)$$

when $(m, n) \neq (\pm 1, 1)$. In this last case,

$$\frac{d}{dT}B_{1,1} = \frac{i}{2}SB_{0,2} + i\frac{\delta}{4}S. \quad (28)$$

Finally, (25) becomes

$$\frac{dS}{dT} + i\sigma S = -iB_{1,1} \quad (29)$$

and the complete spectral system is formed of (27), (28) and (29). With this last relation, $B_{1,1}$ can be eliminated from (28) to give

$$\frac{d^2S}{dT^2} + i\sigma\frac{dS}{dT} - \frac{\delta}{4}S = \frac{1}{2}SB_{0,2},$$

showing that the unstable wave interacts *directly* with only the zonal mode $B_{0,2}$: the minimal truncation is therefore formed of S, $B_{1,1}$ and $B_{0,2}$ and will accordingly be called the *zeroth order truncation.*

Remark. This system is similar to the one found in Pedlosky (1982a,b) when $\delta = 1$ and $\sigma = 0$ in our equations and if dissipation and spatial variations are ignored in his. The comparison is easily made by noticing that his variables P_n, $X_{m,n}$, $Y_{m,n}$ and R are related to ours in the following manner: $B_{0,n} = P_n/2$, $B_{m,n} = X_{m,n} + iY_{m,n}$ and $S \equiv R$. One should also notice that our time scale (the same as in WG) is twice his.

The order $(K+1)$ truncation is defined recursively as all members of the order K truncation to which are added the modes that interact directly with them. Table 1 gives the definition of the order-K truncation for a few orders. One notices that all modes that interact directly or indirectly with the unstable wave are such that $(m+n)$ is even. So, even if they are initially very small, those modes would be recreated by the nonlinear interactions while the others would remain small.

This system has two quadratic global invariants: potential enstrophy and energy. In appendix A, it is shown that conservation of total energy implies that

$$E_T = |S|^2 + 2\sum_{n=1}^{\infty}\frac{B_{0,2n}}{n}$$

is conserved. However, it is shown in appendix B that for truncated systems,

$$E_K = |S|^2 + 2\sum_{n=1}^{L}\frac{B_{0,2n}}{n} \quad (30)$$

TABLE 1.

K (truncation order)	Truncated set
0	$S, B_{1,1}, B_{0,2}$
1	$S, B_{1,1}, B_{0,2}, B_{1,3}$
2	$S, B_{1,1}, B_{0,2}, B_{1,3}, B_{0,4}, B_{2,2}$
3	$S, B_{1,1}, B_{0,2}, B_{1,3}, B_{0,4}, B_{2,2}, B_{3,1}, B_{3,3}, B_{3,5}, B_{1,5}$

is conserved only if the truncation order K is even in which case $L = K/2 + 1$.

Conservation of the potential enstrophy follows immediately from (19). Since

$$\frac{\partial}{\partial T}\langle Q^2\rangle = \frac{\partial}{\partial T}(\langle \zeta^2\rangle - 2\delta\langle Y\zeta\rangle) = 0.$$

This implies that

$$Z = 2\sum_{m,n} |B_{m,n}|^2 - 4\delta \sum_{n=1}^{\infty} \frac{(-1)^{n+1}}{n} B_{0,n}$$

is conserved. This shows that while energy exchanges occurs only between the unstable wave and the zonal part of the flow, all modes are involved when it comes to potential enstrophy partitioning.

It is shown in appendix B that for truncated systems,

$$Z_K = 2\sum_{[m,n]} |B_{m,n}|^2 + 2\delta \sum_{n=1}^{L} \frac{B_{0,2n}}{n} \qquad (31)$$

is also conserved with K even. Here $[m, n]$ means that the sum is carried over the modes that belong to the truncated set. The two summations of (31) can be regrouped in a single one by making the substitution

$$B'_{0,2n} = B_{0,2n} + \frac{\delta}{2n}$$

which brings (31) to

$$Z_K + \frac{\delta^2}{2}\sum_{n=1}^{L} 1/n^2 = 2\sum_{[m,n]} |B'_{m,n}|^2;$$

therefore placing a bound on the growth of the $B_{m,n}$ but none on S. If energy is also conserved in the truncated set as is the case when K is even, S has to be bounded since the $B_{0,2n}$ are; this insures that the truncated system is globally stable. Numerical integrations with odd truncation orders lead to unbounded growth in many cases while the growth was always found to be bounded when the truncation order was even. This does not guarantee that the numerical results are accurate but at least, the truncated system has some properties of the complete one. The results from the numerical integrations presented in the next section were obtained with truncation orders that were always even.

5. Results

A multistep predictor–corrector method was used to integrate (27), (28) and (29); the predictor was a second-order centered difference scheme and the corrector was a fourth-order Adams-Moulton scheme. The initial steps were integrated with a fourth-order Runge-Kutta scheme. Compared to the Runge-Kutta scheme that requires four evaluations per time step and to the second-order centered difference scheme that needs very small time steps, this method was found to be more economical. This is an important factor since we intended to perform integrations at high resolutions i.e. with $K = 128$ which involves 8386 modes.

To test our numerical results, the case where $\delta = 1$ and $\sigma = 0$ was compared against the analytical results found in WG for "subliminal initial conditions" for which the perturbation potential vorticity is initially very small: $B_{1,1}(0) = 0.01$ while all other modes are set to zero. Due to potential vorticity mixing, the analysis of WG shows that the amplitude of the unstable wave should equilibrate at a constant value of $\pi/\sqrt{6}$. Figure 2 shows that for $K = 16$, a truncation similar to the one used in Pedlosky (1982b), the unstable wave oscillates irregularly around the equilibration value. If the resolution is increased to $K = 128$, this oscillation has nearly disappeared and the unstable wave is equilibrating at the correct value.

The absolute potential vorticity fields $Q(X, Y, T)$ for this case are shown at $T = 10$ and 20 on Figs. 3 and 4 when $K = 16$ and 128, respectively. As can be seen, the general picture of the wrap-up of the vorticity is discernible even at low resolution. The low resolution run involves a significant error even on the large scale reflected by the error on $S(T)$. Increasing the resolution to $K = 128$ corrects this deficiency. As may be seen by comparing Fig. 4b with the analytical solution of WG (their Fig. 2c), the latter resolution seems sufficient to give a reasonable picture of what is going on when $\sigma \neq 0$.

Using the same initial conditions as for the case $\sigma = 0$, experiments were conducted with different values of σ and a constant supercritical shear of 1. This means that in all cases, $\delta = 1 + \sigma^2$. Figure 5 shows the evolution in time of $|S(T)|$ when $\sigma = 0.25$, 0.5 and 1.0. In the early stages, the evolution is identical in all cases, the initial conditions and the linear growth rate being the same. In the nonlinear stage, the solutions evolve differently going from a complete equilibration at $\sigma = 0$ towards an oscillatory behavior that becomes more and more pronounced as σ increases. Since the linear phase speed remains constant to a value of $\sigma/2$, the potential vorticity field is then best represented in a

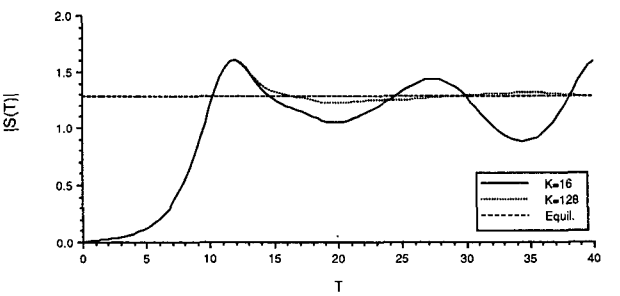

FIG. 2. Evolution in time of $|S(T)|$ for two different truncation orders ($K = 16$ and $K = 128$) when $\sigma = 0$ and $\delta = 1$. The constant level of $|S| = \pi/\sqrt{6}$ corresponding to the equilibration value of Warn and Gauthier (1989) has also been indicated.

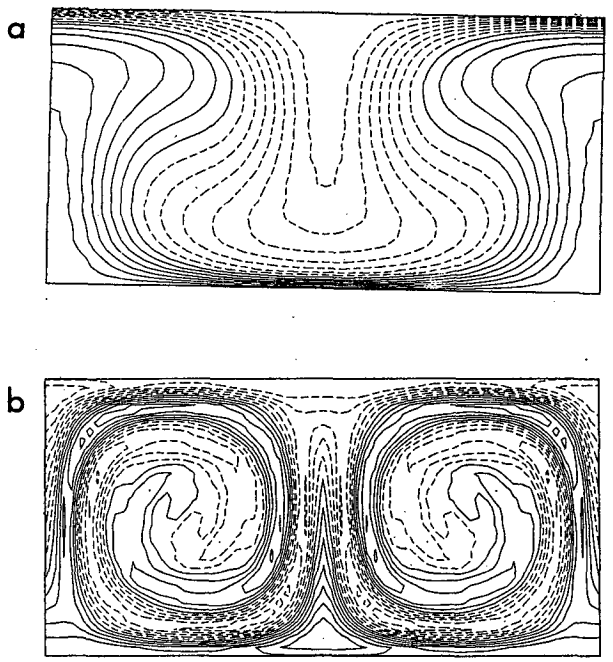

FIG. 3. Absolute potential vorticity field $Q(X, Y, T)$ when $K = 16$ at (a) $T = 10$, (b) $T = 20$. The domain is such that $-\pi/2 < X < 3\pi/2$ and $-\pi/2 < Y < \pi/2$.

reference frame moving with the unstable wave. On Fig. 6, it is shown at $T = 20$ for increasing values of σ. While closed vortices are still developing in the flow, the area over which they extend is shrinking as σ increases and for $\sigma = 4$, no development occurs. Closed

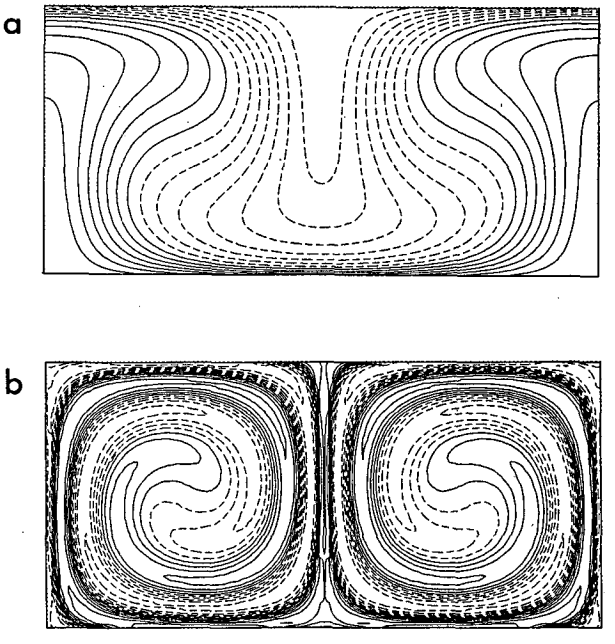

FIG. 4. As in Fig. 3 but for $K = 128$.

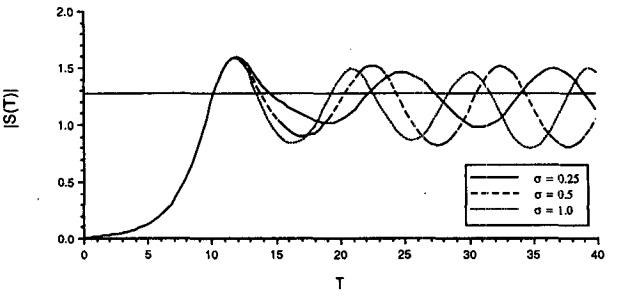

FIG. 5. Evolution of $|S(T)|$ as a function of time for $\delta = 1 + \sigma^2$ and increasing values of σ. The constant level corresponds to the equilibration value when $\sigma = 0$.

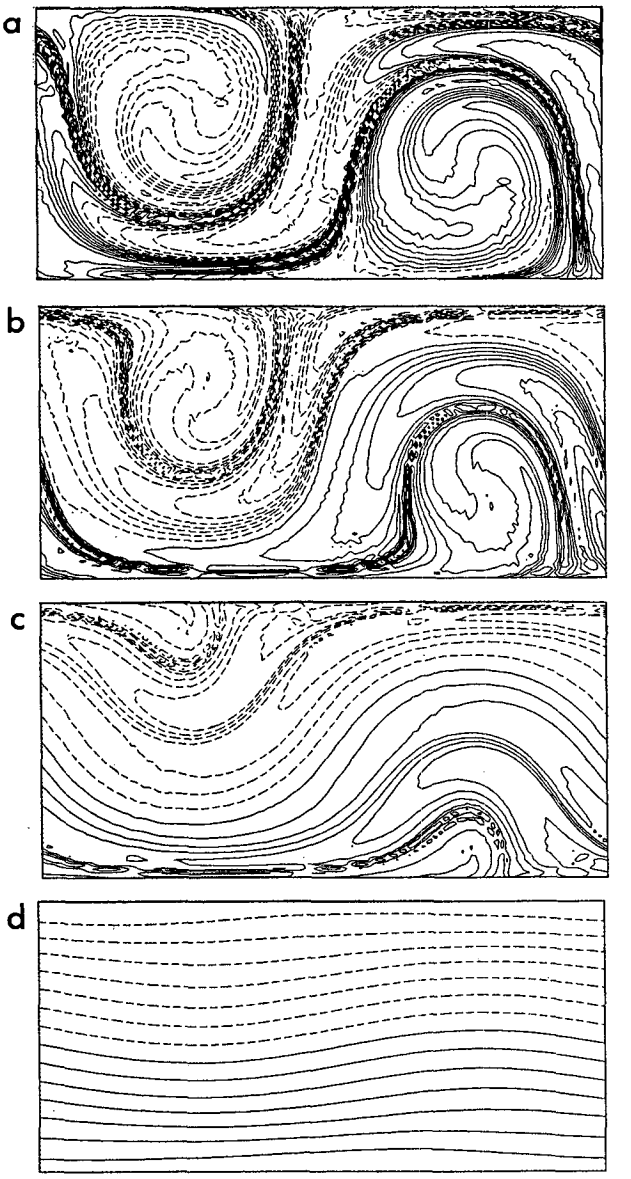

FIG. 6. $Q(\xi, Y, T)$ at $T = 20$ when (a) $\sigma = 0.5$, (b) $\sigma = 1$, (c) $\sigma = 2$, (d) $\sigma = 4$. In all cases, $\delta = 1 + \sigma^2$ and the domain is as in Fig. 1.

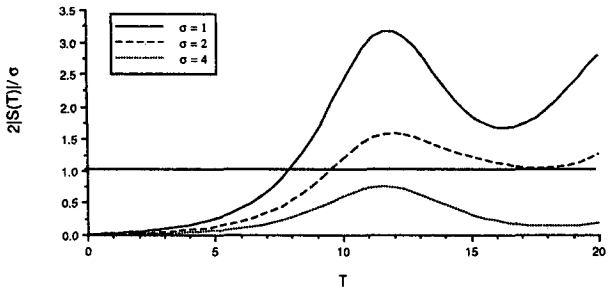

FIG. 7. Plot of $2|S(T)|/\sigma$ as a function of time. Values below 1 indicate that no closed streamlines are present.

vortices would normally be associated with a closed circulation. If $\xi = X - \sigma T/2$, the streamfunction is

$$\psi = \frac{\sigma}{2} Y + |S(T)| \cos\xi \cos Y$$

and closed streamlines are only possible if $|S(T)| > \sigma/2$. It is important to point out that variations in $S(T)$ imply that the pattern of the streamfunction is not steady, its configuration depending on the ratio $2|S(T)|/\sigma$ (see Fig. 1). This ratio has been plotted as a function of time on Fig. 7 for $\sigma = 1$, 2 and 4. It shows that when $\sigma = 4$, closed streamlines never appear and as was observed on Fig. 6d, no closed vortices are present either. The configuration of the vorticity field suggest that a low order model should be a better approximation of the dynamics for this case. To verify this, an experiment using a very low truncation order ($K = 2$) was run and the resulting $|S(T)|$ is in good agreement with the one obtained from the high resolution run (Fig. 8b). By comparison, Fig. 8a shows that when $\sigma = 0$, the low order model becomes inaccurate as soon as the evolution enters its nonlinear stage. Although a substantial improvement is observed, Fig. 8b shows that the two models start again to differ after a finite period of time.

As σ becomes large, one should expect the single wave theory to be a valid approximation to the dynamics (Pedlosky 1970, 1979, 1982a). In that case, the governing equation for $|S(T)|$ would be

$$\frac{d^2|S|}{dT^2} - \frac{|S|}{4}(\delta_S - |S|^2) = 0, \qquad (32)$$

$\delta_S = \delta - \sigma^2$ being the supercritical shear: (32) can be obtained from the spectral equations (27), (28) and (29) truncated at zeroth order. Since δ_S was kept constant in all the experiments reported here, (32) implies that the evolution of $|S(T)|$ is independent of σ. It can also be shown (analytically) that the maximum value attained by $|S|$ is $\sqrt{2\delta_S}$. For $\delta_S = 1$, $|S|_{\max} = \sqrt{2}$, a value that is lower than the maximum of 1.5 attained when $\sigma = 4$. When $\sigma = 10$, Fig. 9 compares the evolution of $|S(T)|$ as predicted by (32) against the result from a high resolution run ($K = 128$): it

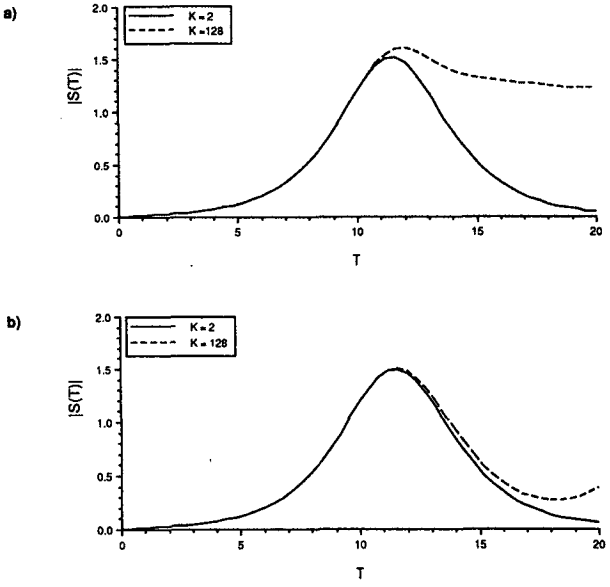

FIG. 8. Evolution in time of $|S(T)|$ for $K = 2$ and $K = 128$ when (a) $\sigma = 0$, (b) $\sigma = 4$. In both cases, $\delta = 1 + \sigma^2$.

indicates very clearly that single wave theory is correct during the time interval $0 \leq T \leq 20$.

In Shepherd (1988), a bound is put on the maximum value of the wavy part of the flow (see eq. (5.6) in his paper): in the present case, this implies that the peak amplitude of $|S|$ must be such that

$$|S|_{\max} \leq \pi\left(\frac{\delta_S + \sigma^2}{3}\right)^{1/2}.$$

For a constant supercritical shear value of 1, this bound implies that when $\sigma = 0$, $|S|_{\max} \leq \pi\sqrt{3}/3 \sim 1.81$. Our results show (see Fig. 2) that $|S|_{\max} \sim 1.60$ which is very close to Shepherd's bound. In all cases, the peak amplitudes are in agreement with his result.

It is important to point out that for inviscid models, the resolution needed to describe a given situation depends on the time period T_S over which an accurate description is required. The results presented here show

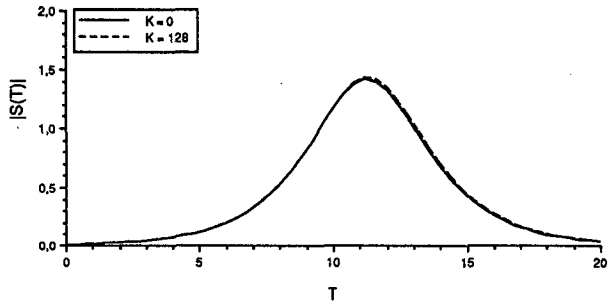

FIG. 9. Evolution in time of $|S(T)|$ for $K = 0$ and $K = 128$ when $\sigma = 10$.

that for a fixed value of T_S, the resolution needed would decrease as σ increases and at some point, the single wave theory would be sufficient. The results show also how one goes from the equilibration due to a complete potential vorticity mixing as in WG to the wave–mean flow interaction model of Pedlosky (1970).

6. Conclusion

The purpose of the present study was to investigate the changes in the dynamics caused by the detuning in the vicinity of the point of minimum critical shear. These issues are of importance when the wavenumber has a continuous spectrum. This is the case when the parameters of the model are not considered to be uniform in space or when the channel is of infinite extent in the zonal direction: this last situation has been considered in the study of the wavepacket problem presented in Pedlosky (1972), Gibbon et al. (1979) and Moroz and Brindley (1984). As pointed out by Pedlosky (1982a), this problem would have to be reformulated to take into account the effect of the nondispersive modes.

When it is set exactly at the point of minimum critical shear, the problem can be solved analytically. In that case, Warn and Gauthier showed that the streamwise potential vorticity mixing leads to the equilibration of the unstable wave. On the other hand (Pedlosky 1982a), when the problem is way off the minimum, the dynamics is that of a weakly unstable wave interacting with the zonal part of the flow and the amplitude $S(T)$ of the unstable wave is then seen to have an oscillatory behavior. Our results show how one goes from one situation to the other. Potential vorticity mixing occurs within the closed vortices but as the detuning σ is increased, their size is decreasing while $|S(T)|$ oscillates with increasing amplitude around a nonzero mean. The emergence of vortices is related to the presence of closed streamlines that exist when the ratio $2|S(T)|/\sigma > 1$. Since the maximum value attained by $|S(T)|$ depends on the supercritical shear, this implies that larger supercritical shears would be necessary for closed vortices to exist as σ increases. However, for σ sufficiently large, one would reach a situation where many unstable waves may coexist: this

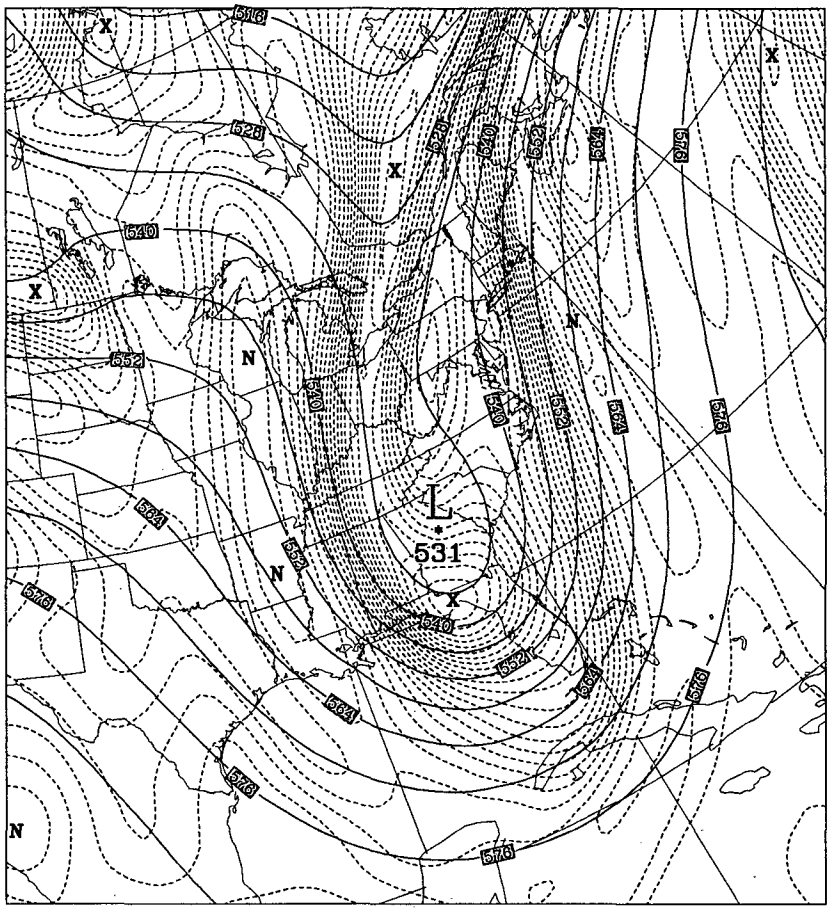

FIG. 10. The 500-mb height field (solid lines) and absolute vorticity (dashed lines) 24 February 1989 on the east coast of North America 0000 UTC.

question has been investigated in other contexts by Hart (1981), Moroz and Holmes (1984), Klein and Pedlosky (1986) and Pedlosky and Polvani (1987). The whole asymptotic analysis presented here would have to be redone for such situations.

The development of strong potential vorticity gradients cannot go on forever; this is, in fact, the limit of validity of the evolution equations as given by (19) and (20). Rhines and Young (1983) mention that those gradients can be destroyed by the presence of diffusion of heat and momentum that becomes important at that point. On the other hand, the emergence of these gradients may very well cause local barotropic instabilities which would lead to horizontal transport of vorticity that would in turn enhance potential vorticity mixing: this point has been studied by Killworth and McIntyre (1985) and Haynes (1985) for the problem of forced barotropic Rossby waves.

One striking feature of our results is the development of strong gradients in the absolute potential vorticity field. This is reminiscent of what is observed in real synoptic systems as can be seen on Fig. 10. It shows the 500-mb height field and the absolute vorticity field on 24 February 1989 on the east coast of North America at 0000 UTC. It clearly indicates that there is a wrap-up of the absolute vorticity field by the 500-mb circulation in a way that resembles the one obtained from our simple model.

Once strong gradients have developed, the evolution enters a fully nonlinear stage that could lead to turbulence. At that point, geostrophic turbulence theory (Salmon 1980) provides another approach to the problem while recent work by Shepherd (1988, 1989) establishes a nonlinear stability theorem that is able to put a bound on the wavy part of the flow. The solutions presented here describe the flow in a transition period when it is going from its marginally stable zonal basic state configuration towards a full nonlinear stage.

Acknowledgments. The author would like to express his gratitude to Prof. T. Warn from the Department of Meteorology at McGill University for suggesting to investigate this aspect of the problem and for many helpful discussions and comments on the manuscript. Thanks are also extended to Ted Shepherd, Joseph Pedlosky and an anonymous reviewer whose comments led to improvements in the final version of the paper. Jean Côté reviewed a preliminary version of the manuscript. This research has been made possible through a Visiting Fellowship in Canadian Government Laboratories from the Natural Sciences and Engineering Research Council of Canada.

APPENDIX A

Conservation of Total Energy

The sum of kinetic and available potential energy in the two-layer system described by (1) is

$$E = \frac{1}{2}(\|\nabla\psi_1\|^2 + \|\nabla\psi_2\|^2 + F(\psi_1 - \psi_2)^2),$$

the *total energy* (see Pedlosky 1979). In terms of the asymptotic expansion used in section 3, the conservation of total energy gives

$$\frac{\partial}{\partial T}(\langle E_0\rangle + \langle E_1\rangle) = 0,$$

at leading order in ϵ, E_0 and E_1 being

$$E_0 = \frac{1}{2}(\|\nabla\psi_1^{(0)}\|^2 + \|\nabla\psi_2^{(0)}\|^2 + F(\psi_1^{(0)} - \psi_2^{(0)})^2),$$

$$E_1 = -\frac{\beta}{\pi F}[Y\psi_1^{(1)} + FY(\psi_1^{(1)} - \psi_2^{(1)})].$$

Using (12) and the definition (19) of the rescaled variable $S(T)$, it is straightforward to show that

$$\langle E_0\rangle = \frac{\beta}{2\pi^2 F}|S|^2. \tag{A1}$$

However, one must know the form of the zonal component of $\psi^{(1)}$ in order to be able to calculate E_1. If $\Phi^{(1)}$ stands for the zonal part of $\psi^{(1)}$, the zonal average of (26) gives

$$\Phi_{2YY}^{(1)} + \frac{F}{\pi^2}(\Phi_1^{(1)} - \Phi_2^{(1)}) = \frac{2}{\pi}\sum_{n=1}^{\infty} B_{0,2n}\sin 2n(Y + \pi/2). \tag{A2}$$

This is not enough to determine $\Phi^{(1)}$. As in Pedlosky (1970), the imposition of a secularity condition at the next order (the removal of an X-independent term that appears in the top layer equation) supplies the required supplementary equation, which is

$$\Phi_{1YY}^{(1)} - F(\Phi_1^{(1)} - \Phi_2^{(1)}) = \frac{|S|^2}{\pi^3}\sin 2(Y + \pi/2). \tag{A3}$$

Solving (A2) and (A3) with the boundary conditions

$$\frac{\partial^2\Phi_n^{(1)}}{\partial T\partial Y} = 0, \quad \text{at} \quad Y = \pm\frac{\pi}{2},$$

the solution is found to be

$$\Phi^{(1)} = 2a(T)e^{\sqrt{F}/2}\sinh\alpha Y\begin{bmatrix}1\\-1\end{bmatrix} - \frac{|S|^2}{8\pi^3(2\pi^2 + F)}\begin{bmatrix}4\pi^2 + F\\F\end{bmatrix}\sin 2(Y + \pi/2) - \frac{1}{4\pi^3}\sum_{n=1}^{\infty}\frac{B_{0,2n}}{n^2(2n^2\pi^2 + F)}\begin{bmatrix}F\\4n^2\pi^2 + F\end{bmatrix} \times \sin 2n(Y + \pi/2), \tag{A4}$$

where $\alpha = (2F)^{1/2}/\pi$ and

$$a(T) = \frac{1}{\sqrt{2F}\,(1 + e^{\sqrt{2F}})} \times \left\{ \frac{|S|^2}{2(2\pi^2 + F)} - \sum_{n=1}^{\infty} \frac{n}{(2n^2\pi^2 + F)} B_{0,2n} \right\}.$$

The introduction of this result in the expression for E_1 gives finally that

$$\langle E_1 \rangle = \frac{\beta}{8\pi^2 F} |S|^2 - \frac{\beta}{4\pi^2 F} \sum_{n=1}^{\infty} \frac{1}{n} B_{0,2n}. \quad \text{(A5)}$$

(A1) and (A5) are combined to give

$$\frac{\partial}{\partial T} \langle E_0 + E_1 \rangle = \frac{\beta}{4\pi^2 F} \frac{\partial}{\partial T} \left(|S|^2 + 2 \sum_{n=1}^{\infty} \frac{1}{n} B_{0,2n} \right)$$

which proves that the spectral quantity

$$E_T = |S|^2 + 2 \sum_{n=1}^{\infty} \frac{1}{n} B_{0,2n}$$

represents the total energy to leading order and is a *global invariant.*

APPENDIX B

Invariants of the Truncated Systems

Referring to Appendix A, the total energy of a system truncated at order K is

$$E_K = |S|^2 + 2 \sum_{n=1}^{L} \frac{1}{n} B_{0,2n} \quad \text{(B1)}$$

where $L = K/2 + 1$ ($L = (K+1)/2$ when K is even (odd). Differentiation of (B1) with respect to T gives

$$\frac{dE_K}{dT} = S^* \frac{dS}{dT} + S \frac{dS^*}{dT} + 2 \sum_{n=1}^{L} \frac{1}{n} \frac{d}{dT} B_{0,2n}. \quad \text{(B2)}$$

From (27), one has that

$$\frac{d}{dT} B_{0,2n} = \frac{i}{2} n[S(B^*_{1,2n+1} - B^*_{1,2n-1}) - S^*(B_{1,2n+1} - B_{1,2n-1})] \quad \text{(B3)}$$

for $n = 1, \cdots, L-1$. Therefore,

$$\frac{d}{dT} \sum_{n=1}^{L-1} \frac{1}{n} B_{0,2n} = \frac{i}{2} (S(B^*_{1,2L-1} - B^*_{1,1}) - S^*(B_{1,2L-1} - B_{1,1})).$$

Using (29), one has

$$S \frac{dS^*}{dT} + S^* \frac{dS}{dT} = iSB^*_{1,1} - iS^* B_{1,1}$$

and (B2) reduces to

$$\frac{dE_K}{dT} = \frac{2}{L} \frac{d}{dT} B_{0,2L} + iSB^*_{1,2L-1} - iS^* B_{1,2L-1}. \quad \text{(B4)}$$

From the definition of a Kth order truncation set,

$$\frac{1}{L} \frac{d}{dT} B_{0,2L} = \frac{i}{2} (-SB^*_{1,2L-1} + S^* B_{1,2L-1})$$

if K is even and (B4) reduces to

$$\frac{dE_K}{dT} = 0.$$

On the other hand, when K is odd (B3) applies with $n = L$ and (B4) becomes

$$\frac{dE_K}{dT} = iSB^*_{1,2L+1} - iS^* B_{1,2L+1} \neq 0.$$

Total energy is therefore conserved only when the truncation order is even.

To show that potential enstrophy is conserved in truncated sets proceeds much in the same way as for the total energy except that the algebra is a little bit more involved. When the truncation order is even, differentiation of (31) with respect to time yields

$$\frac{dZ_K}{dT} = 2 \sum_{[m,n]} \left(B^*_{m,n} \frac{d}{dT} B_{m,n} + \text{C.C.} \right) - \delta |S|^2, \quad \text{(B5)}$$

where (B1) and the fact that E_K is conserved have been used. From (27), one has

$$B^*_{m,n} \frac{d}{dT} B_{m,n} = \frac{i}{4} B^*_{m,n}[(m+n)(SB_{m-1,n+1} + S^* B_{m+1,n+1}) + (m-n)(SB_{m-1,n-1} + S^* B_{m+1,n+1})]. \quad \text{(B6)}$$

The two terms

$$B_{m\mp1,m\pm1} \frac{d}{dT} B^*_{m\mp1,n\pm1}$$

have counterparts of opposite signs to the first two terms of (B6) while

$$B_{m\pm1,n\pm1} \frac{d}{dT} B^*_{m\pm1,n\pm1}$$

generate terms that will cancel the last two. This occurs for all terms except for those related to $B_{1,1}$ who generate some extra terms; it is found that

$$\frac{d}{dT} (B_{1,1} B^*_{1,1} + \text{C.C.}) = \frac{\delta}{2} |S|^2 + \cdots$$

and therefore,

$$\frac{dZ_K}{dT} = 0.$$

REFERENCES

Akylas, T., and D. Benney, 1980: Direct resonance in nonlinear wave systems. *Stud. Appl. Math.*, **63,** 209–226.

——, and ——, 1982: The evolution of waves near direct resonance conditions. *Stud. Appl. Math.*, **67,** 107–123.

Charney, J. G., 1947: The dynamics of long waves in a baroclinic westerly current. *J. Meteor.*, **4,** 135–162.

Eady, E. T., 1949: Long waves and cyclone waves. *Tellus,* **1,** 33–52.

Gibbon, J. D., I. N. James and I. M. Moroz, 1979: An example of soliton behavior in a rotating baroclinic fluid. *Proc. Roy. Soc. Lond.*, **A367,** 219–237.

Guckenheimer, J., and P. Holmes, 1983: Nonlinear Oscillations, Dynamical Systems and Bifurcations of Vector Fields. Springer-Verlag, 453 pp.

Hart, J. E., 1979: Finite amplitude baroclinic instability. *Ann. Rev. Fluid Mech.*, **11,** 147–172.

——, 1981: Wavenumber selection in nonlinear baroclinic instability. *J. Atmos. Sci.*, **38,** 400–408.

Haynes, P., 1985: Nonlinear instability of a Rossby wave critical layer. *J. Fluid Mech.*, **161,** 493–511.

Holopainen, E., 1961: On the effect of friction in baroclinic waves. *Tellus,* **13,** 363–367.

Killworth, P., and M. McIntyre, 1985: Do Rossby wave critical layers absorb, reflect or overreflect? *J. Fluid Mech.*, **161,** 449–492.

Klein, P., and J. Pedlosky, 1986: A numerical study of baroclinic instability at large supercriticality. *J. Atmos. Sci.*, **43,** 1243–1262.

Moroz, I. M., and J. Brindley, 1984: Nonlinear amplitude evolution of baroclinic wave trains and wave packets. *Stud. Appl. Math.*, **70,** 21–62.

——, and P. Holmes, 1984: Double Hopf bifurcation and quasi-periodic flow in a model for baroclinic instability. *J. Atmos. Sci.*, **41,** 3147–3160.

Newell, A., 1972: The post-bifurcation stage of baroclinic instability. *J. Atmos. Sci.*, **29,** 64–76.

Pedlosky, J., 1970: Finite amplitude baroclinic waves. *J. Atmos. Sci.*, **27,** 15–30.

——, 1972: Finite-amplitude baroclinic wave packets. *J. Atmos. Sci.*, **29,** 680–686.

——, 1979: Geophysical Fluid Dynamics. Springer-Verlag, 624 pp.

——, 1982a: Finite-amplitude baroclinic waves at minimum critical shear. *J. Atmos. Sci.*, **39,** 555–562.

——, 1982b: A simple model for nonlinear critical layers in an unstable baroclinic wave. *J. Atmos. Sci.*, **39,** 2119–2127.

——, and L. M. Polvani, 1987: Wave-wave interaction of unstable baroclinic waves. *J. Atmos. Sci.*, **44,** 631–647.

Phillips, N. A., 1954: Energy transformations and meridional circulations associated with simple baroclinic waves in a two-level, quasi-geostrophic model. *Tellus,* **6,** 273–286.

Rhines, P., and W. Young, 1983: How rapidly is a passive scalar mixed within closed streamlines? *J. Fluid Mech.*, **133,** 133–145.

Romea, R. D., 1977: The effects of friction and β on finite-amplitude baroclinic waves. *J. Atmos. Sci.*, **34,** 1689–1695.

Salmon, R., 1980: Baroclinic instability and geostrophic turbulence. *Geophys. Astrophys. Fluid Dyn.*, **15,** 167–211.

Shepherd, T. G., 1988: Nonlinear saturation of baroclinic instability. Part I: the two-layer model. *J. Atmos. Sci.*, **45,** 2014–2025.

——, 1989: Nonlinear saturation of baroclinic instability. Part II: continuously stratified fluid. *J. Atmos. Sci.*, **46,** 888–907.

Stone, P. H., 1978: Baroclinic adjustment. *J. Atmos. Sci.*, **35,** 561–571.

Vallis, G. K., 1988: Numerical studies of eddy transport properties in eddy-resolving and parameterized models. *Quart. J. Roy. Meteor. Soc.*, **114,** 183–204.

Warn, T., and P. Gauthier, 1989: Potential vorticity mixing by marginally unstable disturbances. *Tellus,* **41A,** 115–131.